F. Ismail, P. L. Roe, and H. Nishikawa,
A Proposed Cure to the Carbuncle Phenomenon,
Computational Fluid Dynamics 2006: Proceedings of the Fourth International Conference on Computational Fluid Dynamics, ICCFD, Ghent, Belgium, 10-14 July 2006, Springer 2009.

A Proposed Cure to the Carbuncle Phenomenon

Farzad Ismail[1], Philip L. Roe[2], and Hiroaki Nishikawa[3]

[1] Dept. of Aerospace Engineering, University of Michigan jaymzz@umich.edu
[2] Dept. of Aerospace Engineering, University of Michigan philroe@umich.edu
[3] Dept. of Aerospace Engineering, University of Michigan hiroakin@umich.edu

A new finite volume methodology is introduced to combat the carbuncle. The method features a more accurate treatment of entropy in the flux formulation at the cost of a small computational overhead. This new flux function is tested on a hypersonic flow past a circular cylinder on both structured quadrilateral and unstructured triangular grids, producing encouraging results.

1 Introduction

Numerical shock prediction is a very important aspect of computing aerodynamic flows, and shock capturing finite-volume methods are commonly used to predict shocks in various situations with considerable success. However, it seems that most shock capturing methods fall short in predicting very strong shocks, which is a crucial element in designing hypersonic vehicles. Except for a few notoriously diffusive schemes ([21] and the simplest version of Harten-Lax-van Leer [7], most schemes[4] exhibit some form of anomaly when predicting strong shocks. The commonest of these is the carbuncle phenomenon, produced when computing a hypersonic flow past a blunt body such as a circular cylinder. Instead of having a smooth bow shock profile upstream of the cylinder, the solution features a pair of oblique shocks ahead of the stagnation region (Fig 2). Such a solution is actually a true solution of the Euler equations, and can even be produced experimentally [2]. Many have proposed cures to the carbuncle problem [15], [14], [12], [13], [11], [3], [20] but none are universally accepted, and most papers begin by criticizing previous work.

The most common view follows Quirk [16] in supposing that the carbuncle manifests a two-dimensional numerical instability of the Euler equations, often

[4] There are proposals to adopt a hybrid of very dissipative and less dissipative fluxes, deploying the former near the shock and the latter away from shock but the basis of the switch is somewhat ad hoc. Furthermore, it is not clear how any switch would work for complex problems like shock-boundary layer interactions or shock-contact interactions.

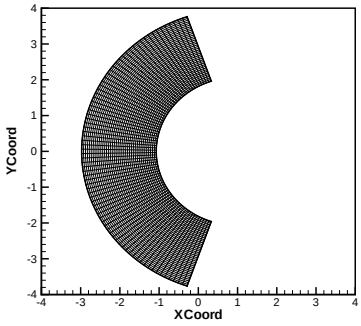

Fig. 1. Quadrilateral grids on a circular cylinder with 80 x 160 cells.

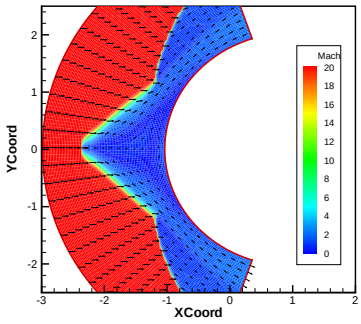

Fig. 2. Results of the original Roe flux with M=20. Contours of Mach number and velocity vectors.

supposed to be an odd-even decoupling. However, Roe *et al* point out that the phenomenon occurs at all frequencies and that a version can be found in one dimension. If the physical viscosity is included as in the Navier-Stokes equations, the tendency to form a carbuncle is reduced, but it disappears only at very low Reynolds number [14]. Nor does it help to include the real gas effects that would accompany very strong shocks in the real world [4], [5], [6].

Here, we propose to combat the carbuncle phenomenon by strongly enforcing entropy stability. First, we will describe some motivating discoveries.

2 The Root of the Carbuncle ?

A simple setting for the carbuncle phenomenon, proposed by [3], is a steady one-dimensional shock on a rectangular two-dimensional grid. Such a carbuncle evolves in three universal but distinct stages: "pimples", "bleeding" and "carbuncle" [17]. The "pimples" are an initial instability largely confined to the vicinity of the shock, whereas the "bleeding" sees these instabilities propagated downstream as layers of alternately high and low velocity. After sufficient amplification the low velocities develop regions of reversed flow that break out ahead of the shock to form the "carbuncle". The second and third stages weakly satisfy the Euler equations but are only observed experimentally in some artificial setup. Accordingly, we seek to prevent the instability at the pimple stage, by improving the basic process of shock-capturing.

Since anomalies appear in both entropy and vorticity, Ismail[9] investigated preventing the carbuncle by controlling either vorticity or entropy. He found vorticity control to be ineffective, so we focus here on control of entropy. Also, even in one dimension, very strong shocks can be unstable both in the sense of entropy [1], and in spontaneous relocation [18], which suggests a link.

3 The Entropy-Stable (ES) Flux

Entropy stability can be studied in one dimension by applying a finite volume method to the conservation laws $\partial_t \mathbf{u} + \partial_x \mathbf{f}(\mathbf{u}) = 0$. Semi-discrete entropy conservation requires [22, 1]. the numerical interface flux $\mathbf{f}^*$ to satisfy $[\mathbf{v}]^T \mathbf{f}^* = [\rho u]$ where $\mathbf{v} = (\frac{\gamma - s}{\gamma - 1} - \frac{1}{2}\frac{\rho}{p}(u^2), \frac{\rho u}{p}, -\frac{\rho}{p})^T$ are the entropy variables[5] and the square bracket denotes a difference operator. The following *entropy-conservative* flux [18] is explicit and numerically well-formed.

$$\mathbf{f}^* = \begin{bmatrix} \hat{\rho}\hat{u} \\ \hat{\rho}\hat{u}^2 + \hat{p_1} \\ \hat{\rho}\hat{u}\hat{H} \end{bmatrix} = \mathbf{f}_C \tag{1}$$

The quantities $\hat{(\cdot)}$ are averaged quantities at the flux-interface satisfying

$$\begin{aligned} \hat{\rho} &= \bar{z_1} z_3^{ln}, & \hat{u} &= \frac{\bar{z_2}}{\bar{z_1}}, & \hat{p_1} &= \frac{\bar{z_3}}{\bar{z_1}} \\ \hat{p_2} &= \frac{\gamma + 1}{2\gamma}\frac{z_3^{ln}}{z_1^{ln}} + \frac{\gamma - 1}{2\gamma}\frac{\bar{z_3}}{\bar{z_1}}, & \hat{H} &= \frac{1}{2}\hat{u}^2 + \frac{\gamma}{\gamma - 1}\frac{\hat{p_2}}{\hat{\rho}} \end{aligned} \tag{2}$$

where $^{\bar{}}$ and ^{ln} represent arithmetic and logarithmic[6] means [18] and

$$z_1 = \sqrt{\frac{\rho}{p}}, \qquad z_2 = \sqrt{\frac{\rho}{p}}u, \qquad z_3 = \sqrt{\rho p} \tag{3}$$

To ensure that entropy is generated with the correct sign, we add upwind terms to give the *entropy-stable* flux (one for which $[\mathbf{v}]\mathbf{f}^* \leq \mathbf{0}$)

$$\mathbf{f}^*(\mathbf{u}_L, \mathbf{u}_R) = \mathbf{f}_C(\mathbf{u}_L, \mathbf{u}_R) - \frac{1}{2}\hat{\mathbf{R}}|\hat{\mathbf{\Lambda}}\hat{\mathbf{S}}|\hat{\mathbf{R}}^{\mathbf{T}}[\mathbf{v}] \tag{4}$$

where $\mathbf{R}$ and $\mathbf{\Lambda}$ denote the right eigenvectors and the diagonalized eigenvalues of the Euler equations. The scaling factor $\mathbf{S} = diag(\frac{\rho}{2\gamma}, \frac{(\gamma-1)\rho}{\gamma}, \frac{\rho}{2\gamma})$ relates to the differential identity [1], $\mathbf{R}^{-1} d\mathbf{u} = \mathbf{S}\mathbf{R}^T d\mathbf{v}$. The new flux function coincides to second order accuracy with the original Roe-flux[7], but is additionally constrained to capture exactly pure contact discontinuities of any strength. This property, which guarantees accuracy in boundary layers, has sometimes been thought to induce carbuncles. To enforce the contact-capturing property [18], the averaged speed of sound must be evaluated from $\hat{a} = (\frac{\gamma \hat{p_1}}{\hat{\rho}})^{\frac{1}{2}}$ and the density averaged using a logarithmic mean. Based on these restrictions and for computational economy, it was proposede in [9] that the averages in the dissipative flux are *exactly* the averages in the entropy-conserving flux.

[5] This is the only choice of entropy variables that can be used in the Navier Stokes equations [8] and $s = \ln p - \gamma \ln \rho$ is the physical entropy.

[6] The logarithmic mean is here defined as $L(x, y) = (x - y)/(\ln x - \ln y)$, and has an efficient series representation if $x \simeq y$.

[7] Recall that the original Roe-flux [19] is $\mathbf{f}^* = \bar{\mathbf{f}} - \frac{1}{2}\hat{\mathbf{R}}|\hat{\mathbf{\Lambda}}|\hat{\mathbf{R}}^{-1}[\mathbf{u}]$

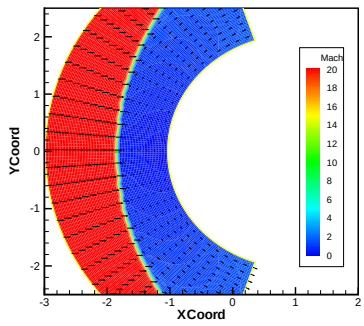

Fig. 3. The ES flux at M=20, on the grid of Figures 1 and 2.

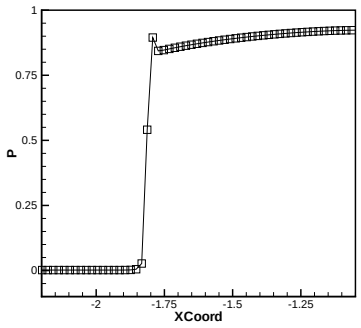

Fig. 4. Spurious overshoots of pressure along the centerline.

For conciseness, we have only presented the flux-function in one dimension. However, because it is a finite volume method, the extension to arbitrary grids in higher dimensions is straightforward (for details see [9]).

4 Numerical Results

The test case is the steady-state flow past a two dimensional cylinder. Various grids and Mach numbers have been employed; a typical structured quadrilateral grid is shown in Figure 1. In all cases reported here, we used a first order explicit method with $\nu = 0.2$ and the code was run until the residual is of $O(10)^{-8}$. Second-order results were reported in [9]. All of our results for structured grids indicate that results from the entropy-stable flux (for example Figure 3) are quite free of the carbuncle phenomenon. However, the shock profile is slightly broader with the introduction of a few intermediate cells (Fig.4) and this may be the price we have to pay.

Previous studies [3] suggest that the carbuncle can be made to appear if the cell aspect is increased, with the short dimension parallel to the shock. This is consistent with a view that one needs numerical damping in the tangential direction. However, our entropy-stable computations were not sensitive to this aspect of the grid (compare Figures 5 and 6 with Figure 3).

Also, the profile around the shock exhibits spurious oscillations. This is because our flux function guarantees only the correct sign of entropy production but not necessarily the correct amount. The actual production is of order δ^2 whereas the required production is of order δ^3. To achieve monotonicity, a flux function must generate 'enough' entropy production across a shock. Flux functions that have this property are called *entropy-consistent (EC)* fluxes[18]. We therefore modify the eigenvalues of equation (4) such that $|\hat{\mathbf{\Lambda}}| = |\hat{\mathbf{\Lambda}}| + \alpha[|\mathbf{\Lambda}|]$

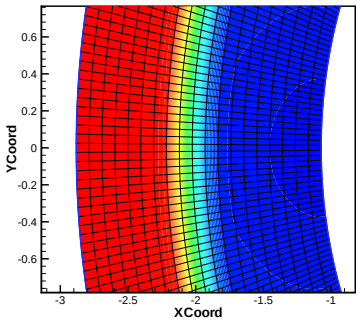

Fig. 5. ES flux with 20 x 200 cells.

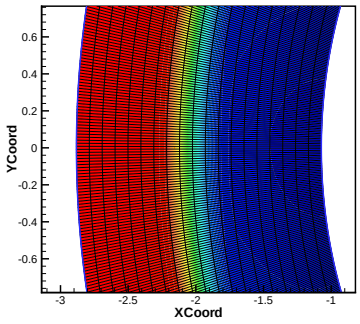

Fig. 6. ES flux with 20 x 600 cells.

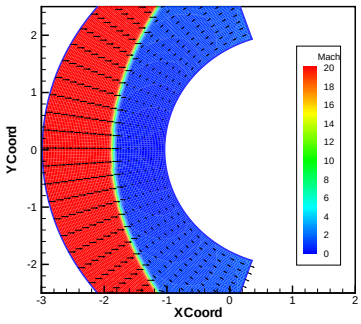

Fig. 7. EC-flux at M=20.

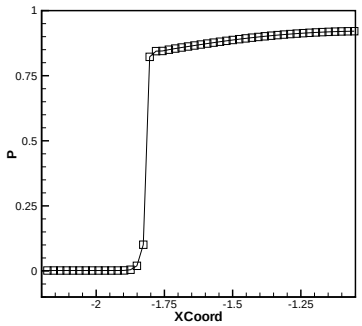

Fig. 8. Pressure profile of EC-flux.

[10]. For the choice of $\alpha = 0.2$, the entropy-consistent flux produces monotone, carbuncle-free solutions on quadrilateral grids (Figs. 7-8).

However, the carbuncle is not yet vanquished. On unstructured triangular grids, such as Figure 9, we discovered that it is produced even by the entropy-consistent flux (although in less severe form than the regular flux). It seems to be reduced (rather surprisingly, and at the expense of increasing spurious overshoots) if we choose smaller values of α and is least when $\alpha \to 0$. This strongly suggests that entropy stability is not the only cause of carbuncles. One possibility may lie in the nature of the finite-volume method itself, with its reliance on pairwise interactions between cells, and therefore merely one-dimensional physics. This may be responsible for the shock being very sharp but poorly aligned.In fact, a better solution can be obtained by creating a better alignment of the grid with the shock, although we do not have sufficient space to show these results. Analysis in [18] offers the possibility of multidimensional extensions, that should be less dependent on the grid.

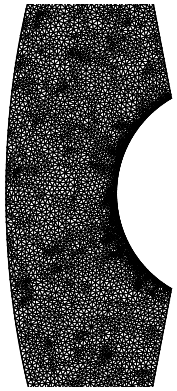

Fig. 9. An unstructured grid.

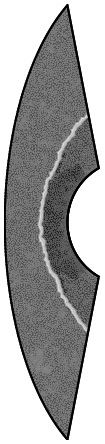

Fig. 10. ES flux on the grid of Figure 9.

References

1. Barth, T. In *Num. Meth. for Gasdyn. Syst. On Unstructured Meshes*. 1999.
2. Bogdonoff, S., and Vas, I. *J. Aero. Sci 26* (1959), 584.
3. Dumbser, M., Moschetta, J., and Gressier, J. *JCP 197* (2004), 647.
4. Edwards, J. In *CFD Conference* (2001), no. A01-31131, AIAA Conference.
5. Gnoffo, P. *Ann. Rev. Fluid Mech. 31* (1999), 459–494.
6. Gnoffo, P., and White, A. No. 2004-2371, AIAA Thermophysics Conference.
7. Harten, A, Lax, P.D. and van Leer, B., *SIAM Review* (1983)
8. Hughes, T. *Comp. Meth. App. Mech. Eng. 54* (1986).
9. Ismail, F. PhD thesis, The University of Michigan, 2006.
10. Ismail, F., and Roe, P. *in preparation for JCP*.
11. Kim, S.-s., Kim, C., Rho, O.-H., and Hong, S. *JCP 186* (2003), 342.
12. Lin, H.-C. *JCP 117* (1995), 20–27.
13. Liou, M. *JCP 160* (2000), 623–648.
14. Pandolfi, M., and d'Ambrosio. *JCP 166* (2001), 271–301.
15. Peery, K., and Imlay, S. No. 88-2924, AIAA Conference.
16. Quirk, J. *Int. J. Num. Meth. Fluids 18* (1994), 555–574.
17. Roe, Nishikawa, Ismail, and Scalabrin. No. 2005-4872, AIAA Conference.
18. Roe, P. *to be published in JCP*.
19. Roe, P. *J. Comp. Physics 43* (1981), 357–372.
20. Sanders, R., Morano, E., and Druguet, M. *JCP 54* (1994).
21. Steger, J., and Warming, R. *JCP 40* (1981), 263–293.
22. Tadmor, E. In *Acta Numerica*. 2002.